Microscopic origin of local moments in a zinc-doped high-T_c superconductor

X. L. Qi and Z. Y. Weng
Center for Advanced Study, Tsinghua University, Beijing 100084, China
(Dated: February 2, 2008)

The formation of a local moment around a zinc impurity in the high-T_c cuprate superconductors is studied within the framework of the bosonic resonating-valence-bond (RVB) description of the $t-J$ model. A topological origin of the local moment has been shown based on the phase string effect in the bosonic RVB theory. It is found that such an $S = 1/2$ moment distributes near the zinc in a form of staggered magnetic moments at the copper sites. The corresponding magnetic properties, including NMR spin relaxation rate, uniform spin susceptibility, and dynamic spin susceptibility, etc., calculated based on the theory, are consistent with the experimental measurements. Our work suggests that the zinc substitution in the cuprates provide an important experimental evidence for the RVB nature of local physics in the original (zinc free) state.
PACS numbers: 74.20.Mn,74.25.Ha,75.20.Hr

I. INTRODUCTION

The Zn substitution of the in-plane Cu^{2+} ions in the high-T_c cuprates introduces some novel properties to the system. Although a Zn^{2+} ion can be considered as a nonmagnetic impurity in the CuO_2 plane, strong magnetic signatures have been detected at the surrounding Cu sites. The NMR and NQR experiments[1,2,3,4,5] have shown the presence of staggered antiferromagnetic (AF) moments near the Zn site, whose sum behaves like an $S = 1/2$ magnetic moment as indicated by a Curie-like $1/T$ behavior in both the spin-lattice relaxation rates and Knight shift at low temperatures. The STM experiments have revealed[6] a sharp near-zero-bias peak around the Zn site, where the quasi-particle coherent peak, appearing near the superconductivity gap in the bulk case, is suppressed simultaneously. The zinc replacement has also shown a strong destructive effect on T_c, and only several percentage of zinc doping can fully destroy the bulk superconductivity[7].

In order to explain the STM experiment beyond a conventional nonmagnetic impurity scattering treatment[8], the existence of a local magnetic moment has been *assumed*, whose interaction with the d-wave nodal quasiparticles leads to a Kondo resonance peak[9,10,11,12]. Theoretically it remains a great challenge to understand the microscopic origin of the magnetic moment found near a nonmagnetic Zn impurity. In one of recent attempts, it was interpreted[13] as due to the binding of an $S = 1/2$ nodal quasi-particle to the impurity, based on a modified mean-field theory of the $t - J$ model. The local staggered AF moments were also explained[14] as a local spin-density-wave (SDW) ordering. But there still lacks a unified theory that can self-consistently explain the free moment and local AF ordering near the zinc impurity without suffering a magnetic instability. Nonetheless, various approaches have at least indicated that the zinc phenomena are quite different from those caused by nonmagnetic impurities in a conventional superconductor and have something directly to do with the nature of the underlying doped Mott insulators. A good understanding of the pure strongly correlated system, therefore, is quite essential in order to sensibly address the overall zinc impurity issue.

In this paper, we approach the zinc problem by using a microscopic description of doped Mott insulators, in which AF correlations in spin degrees of freedom are systematically described at various ranges as a function of doping concentration of holes. We show that an $S = 1/2$ moment does emerge, naturally, near a zinc impurity, which is physically originated from an RVB pair in the original spin background. The latter becomes unpaired upon the Zn substitution, with one of its constituent spin being removed, together with the underlying Cu^{2+} ion. In particular, we find that such an $S = 1/2$ moment cannot escape from the zinc impurity due a topological reason. It is a consequence of the nonlocal mutual entanglement between spin and charge degrees of freedom known as the phase string effect. Due to this effect, a neutral spin-1/2 excitation (spinon) always carries a fictitious π fluxoid as seen by the charge carriers and, what is more, even a vacancy on the lattice, such as a zinc impurity, also acts as a vortex when the charge carriers are condensed. Consequently, the condensate cannot survive in the presence of a zinc impurity unless a spin 1/2, which carries an antivortex, is trapped nearby to compensate the vortex effect.

In this bosonic RVB description, we show that the induced $S = 1/2$ moment around the zinc impurity distributes like staggered AF moments due to the short-range AF correlations already present in the spin background, which are frozen into a local AF ordering once the direction of the moment is fixed, say, by external magnetic fields. The calculated NMR spin-lattice relaxation rates and uniform spin susceptibility are found to be in a systematic agreement with the experiments. The midgap spin excitations are also investigated, with the results consistent with the neutron experiment[15].

An important fact that we find is that all these novel properties are already exhibited in a zinc-doped state obtained by a 'sudden approximation': simply removing a spin sitting at the zinc site from the original pure system. A self-consistent adjustment of the RVB background beyond such a sudden approximation only further strength-

ens the local trapping of the $S = 1/2$ moment as well as local AF staggered ordering around the impurity. Therefore, a Zn impurity in the high-T_c cuprates constitutes a *direct* probe of the *pure* system according to the present theory. Namely, both the local $S = 1/2$ moment and the staggered AF moments 'induced' by a zinc substitution truthfully mirror the nature of the original doped Mott insulator. In this sense, the zinc substitution simply reveals the 'secrets' of local physics already hidden in the zinc-free ground state.

The remainder of the paper is organized as follows. In Sec. II, we present the topological reason that ensures an $S = 1/2$ moment being trapped around a zinc impurity, based on the phase string effect in the bosonic RVB description of the $t-J$ model. Then in Sec. III, we present a generalized mean-field description for the doped Mott insulator with a zinc impurity. The detailed numerical results are given in Sec. IV. Finally, Sec. V is devoted to conclusions and discussion.

II. TOPOLOGICAL ORIGIN OF THE LOCAL MOMENT AROUND A ZN IMPURITY

A. Bosonic RVB framework

We start with an effective description of the *pure* system of a doped Mott insulator, obtained[17,18] based on the $t-J$ model in an all-boson representation (i.e., the phase-string formalism).

The effective Hamiltonian is given by[17,18] $H_{eff} = H_h + H_s$, with

$$H_h = -t_h \sum_{\langle ij\rangle} h_i^\dagger e^{i\left(A_{ij}^s - \phi_{ij}^0\right)} h_j + h.c. \tag{1}$$

$$\begin{aligned} H_s &= -\frac{J}{2}\sum_{<ij>\alpha} \Delta_{ij}^s e^{i\alpha A_{ij}^h} b_{i\alpha}^\dagger b_{j-\alpha}^\dagger + h.c. \\ &+\frac{J}{2}\sum_{<ij>} \left|\Delta_{ij}^s\right|^2 + \lambda\left(\sum_{i,\alpha} b_{i\alpha}^\dagger b_{i\alpha} - N(1-\delta)\right) \end{aligned} \tag{2}$$

where $h_i^\dagger$ and $b_{i\alpha}^\dagger$ denote the creation operators of bosonic holons and spinons, respectively, and Δ_{ij}^s is the bosonic RVB order parameter determined either self-consistently or by minimizing the free energy. In the pure system, a uniform solution, $\Delta_{ij}^s = \Delta^s$, [$ij \in$ the nearest-neighbor (nn) sites], is usually obtained[18]. The Lagrangian multiplier λ in (2) is introduced to enforce the global constraint of the total spinon number:

$$\sum_{i,\alpha} \left\langle b_{i\alpha}^\dagger b_{i\alpha} \right\rangle = N(1-\delta). \tag{3}$$

A unique feature in this model is the topological gauge field A_{ij}^s, ϕ_{ij}^0, and A_{ij}^h, defined on a nn link (ij), as follows:

$$A_{ij}^s = \frac{1}{2}\sum_{l\neq i,j} \left[\theta_i(l) - \theta_j(l)\right] \left(\sum_\sigma \sigma n_{l\sigma}^b\right), \tag{4}$$

$$\phi_{ij}^0 = \frac{1}{2}\sum_{l\neq i,j} \left[\theta_i(l) - \theta_j(l)\right], \tag{5}$$

and

$$A_{ij}^h = \frac{1}{2}\sum_{l\neq i,j} \left[\theta_i(l) - \theta_j(l)\right] n_l^h. \tag{6}$$

Here $n_{l\sigma}^b$ and n_l^h are spinon and holon number operators, respectively. By noting $\theta_i(l) = \mathrm{Im}\ln\left(z_i - z_l\right)$ with $z_i = x_i + iy_i$ representing the complex coordinate of a lattice site i, one has

$$\sum\nolimits_C A_{ij}^s = \pi \sum\nolimits_{l\in\Sigma_C} \left(n_{l\uparrow}^b - n_{l\downarrow}^b\right), \tag{7}$$

$$\sum\nolimits_C A_{ij}^h = \pi \sum\nolimits_{l\in\Sigma_C} n_l^h, \tag{8}$$

and ϕ_{ij}^0 is a uniform π-flux gauge field, satisfying

$$\prod_{\square} e^{i\phi_{ij}^0} = -1 \tag{9}$$

for each plaquette. It means that each holon behaves like a π fluxoid through A_{ij}^h, which is felt by spinons in H_s (here C denotes a closed loop and Σ_C is the area encircled by it), and *vice versa*. Thus holons and spinons are mutually frustrated by each other nonlocally via the topological fields, A_{ij}^s and A_{ij}^h, which represents the phase string effect hidden in the $t-J$ model.

In this description, the superconducting state is realized by the holon condensation, $\langle h^\dagger\rangle \equiv h_0 \neq 0$, while spinons remain RVB paired as characterized by $\Delta^s \neq 0$. Specifically, the superconducting order parameter can be written as[18,19]

$$\Delta^{\mathrm{SC}} = \Delta^0 e^{i\Phi^s} \tag{10}$$

where $\Delta^0 \propto \Delta^s h_0^2$, and Φ^s is defined by

$$\Phi_i^s \equiv \sum_{l\neq i} \theta_i(l) \left(\sum_\alpha \alpha n_{l\alpha}^b\right) \tag{11}$$

which describes that each spinon carries a 2π vortex in the phase of Δ^{SC} (known as a spinon-vortex[19]). Since spinons form singlet RVB pairs, these vortices and antivortices are generally cancelled out in (11) such that the phase coherence of Δ^{SC} can be established at low temperatures[18,19].

A non-superconducting state, with a finite pairing amplitude Δ^0 but is short of phase coherence, can be realized at higher temperatures where excited spinons disorder the phase Φ_i^s according to (11). Such a low-temperature pseudogap phase is called spontaneous vortex phase due to the presence of free spinon-vortices at

$T_c < T < T_v$[19]. The high-temperature pseudogap phase is defined at $T_v < T < T_0$, where the holon condensation is gone such that the pairing amplitude $\Delta^0 = 0$, whereas the RVB order parameter Δ^s still remains finite. The latter vanishes beyond T_0.

The following discussion of local moments around zinc impurities will be mainly focused in the superconducting phase and spontaneous vortex phase, where the relation (10) generally holds with $\Delta^0 \neq 0$.

B. Topological origin of local moments

Now let us consider a zinc impurity added to a pure system of the doped Mott insulator described by the bosonic RVB theory outlined above.

In the high-T_c cuprates, chemically it is a Cu^{2+} ion that is replaced[16] by a Zn^{2+}. A Zn-potential may be considered as a unitary potential[8] which pushes away *both* spin and charge from the zinc site. In the framework of the $t-J$ model, a zinc impurity can be thus simply treated as an *empty* site with excluding the occupation of any electrons.

Since a zinc impurity does not change the total charge of the system in the substitution of a Cu^{2+} ion by a Zn^{2+}, one may construct an effective theory by starting with that for a *pure* system and removing a neutral spin (spinon) from the system. A heuristic procedure is to imagine exciting a spinon at the would-be zinc site. With its spin being 'fixed', its exchange coupling with the surrounding spins is effectively cutoff. Nor a holon can hop to this site due to the no-double-occupancy constraint in the $t-J$ model. Whether one removes or not such an isolated spin, the effective effect of a zinc impurity is created at such a site.

Based on the bosonic RVB theory, corresponding to the creation of an isolated spinon at the would-be zinc site, a 2π vortex will then appear in the superconducting order parameter (10) via Φ^s or a π vortex in the holon Hamiltonian (1) via A^s_{ij}, in the superconducting or spontaneous vortex phase with the condensation of holons, $\langle h^\dagger \rangle \neq 0$. In other words, each zinc impurity will always induce a nonlocal response (vortex current) from the charge condensate as shown in Fig. 1(a).

Such a topological effect of a zinc impurity can be traced back to the nonlocal effect in the pure system of such a doped Mott insulator, known as the phase string effect: the motion of doped holes will always create string-like sign defects which cannot be 'repaired' at low energy in the $t-J$ model[17]. Consequently spin and charge degrees of freedom are mutually 'entangled' in the pure system. An 'empty' (zinc) site then can be nonlocally perceived by the charge degrees of freedom to result in the above vortex-like response centered at this site.

A more rigorous derivation is to start from the phase string representation[17] of the $t-J$ model with the presence of an 'empty' site. Under the same RVB order parameter Δ^s_{ij}, one obtains essentially the same effective Hamiltonians, (1) and (2), except for that in (5) the summation does not include the 'empty' (zinc) site, denoted by i_0. Namely,

$$\begin{aligned} \phi^0_{ij} &\rightarrow \phi^0_{ij} - \phi^{\rm Zn}_{ij} \\ \phi^{\rm Zn}_{ij} &= \frac{1}{2}\left[\theta_i(i_0) - \theta_j(i_0)\right]. \end{aligned}$$

Note that the summations in (4) and (6) should also exclude the zinc site, which are automatically ensured since both spinons and holons are not allowed at the site i_0, so that the definitions for A^s_{ij} and A^h_{ij} remain the same as in the pure system. By noting

$$\sum\nolimits_C \phi^{\rm Zn}_{ij} = \pi$$

for a closed loop around i_0, one finds that a zinc site is bound to an extra π-fluxoid which will always induce a vortex current in (1) if the holons are condensed. Similarly, using the original definition of Δ^0 in (10), the effect of an empty site can be reexpressed by the replacement $\Delta^0 \rightarrow \Delta^0 e^{i\Phi^0_{i_0}}$, with $\Phi^0_{i_0}$ giving rise to a 2π vortex. Both are consistent with the previous argument based on freezing a spinon at the site i_0, which also lead to Fig. 1(a).

Now it is natural to see why a zinc impurity will generally induce a spin-1/2 around it in the superconducting and spontaneous vortex phases. In the superconducting state, a Zn-vortex costs a logarithmically divergent energy and thus must be 'screened' by nucleating a neutral $S = 1/2$ spinon which carries an antivortex[19] and is bound to the latter, as shown in Fig. 2b. Note that in the pure system, an isolated spinon excitation is not allowed in the superconducting bulk state due to the same reason, and only spinons in bound pairs (vortex-antivortex pairs) can be excited, which is known as the spinon confinement[19]. It is also noted that in a different approach[20] based on a similar all-boson formalism, an 'unscreened' current vortex is predicted around a zinc impurity *if* the $S = 1/2$ is trapped around which carries such a (anti)vortex. By contrast, such a (anti)vortex is always compensated in the present approach since a zinc impurity itself also induces a vortex as shown in Fig. 1(a).

In the spontaneous vortex phase, even though free vortices are thermally present in the bulk in a similar fashion as in Kosterlitz-Thouless transition, there still exists a logarithmic attraction between a Zn-vortex and a spinon-vortex at short-range, and a bound state (although not a confined state below T_c) between a Zn and an $S = 1/2$ moment can be still present below T_v.

Therefore, there is a fundamental topological reason for an $S = 1/2$ moment to be trapped around a zinc impurity in the bosonic RVB theory of doped Mott insulators, in the superconducting and spontaneous vortex phases.

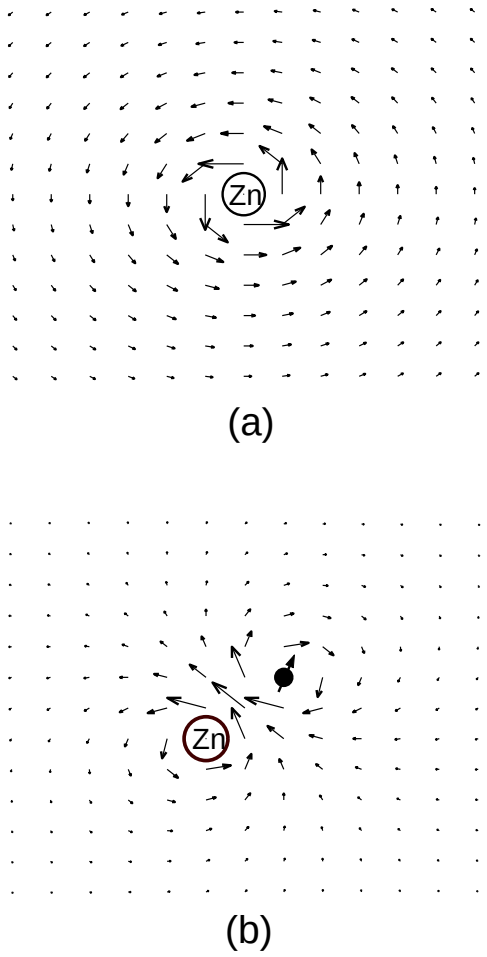

FIG. 1: (a) A vacancy (zinc impurity) always induces a vortex-like supercurrent response in the superconducting phase due to the phase string effect. (b) To compensate such a vortex effect, a spinon, which carries an antivortex, has to be trapped around the zinc impurity, giving rise to a local $S = 1/2$ moment.

III. GENERALIZED MEAN-FIELD DESCRIPTION

Once we have established the topological origin of the $S = 1/2$ moment around a zinc impurity, a simple effective description of the system with one zinc impurity can be developed.

Note that after trapping a spinon nearby, the vortex induced by the zinc impurity is compensated by the antivortex carried by the spinon, as illustrated by Fig. 1(b). Then the system is topologically trivial at a distance sufficiently away from the impurity where the system remains the same as the pure system. The change of the state mainly occurs around the impurity with a characteristic scale comparable to the spin correlation length.

We can construct a state based on the ground state $|\Psi_0\rangle$ of the pure system, by removing a *local* spin sitting at the site i_0, denoted by

$$|\Psi_0\rangle_{\rm Zn} \equiv \hat{P}_{i_0} |\Psi_0\rangle . \tag{12}$$

To leading order approximation, $|\Psi_0\rangle_{\rm Zn}$ may be regarded as a 'sudden approximation' of the true ground state $|\Psi\rangle_{\rm Zn}$ in the presence of a zinc. Both have the same spin and charge quantum numbers. By 'suddenly' removing a spinon at i_0, its original partner spinon in $|\Psi_0\rangle$ will be left around the site i_0 in $|\Psi_0\rangle_{\rm Zn}$ within the spin correlation length ξ. At distances larger than ξ, on the other hand, $|\Psi_0\rangle_{\rm Zn}$ is essentially the same as $|\Psi_0\rangle$. Due to the topological reason discussed in last section, the free spinon partner created in $|\Psi_0\rangle_{\rm Zn}$ should remain trapped around the impurity. Therefore one expects $|\Psi_0\rangle_{\rm Zn}$ to have a good overlap with the true ground state $|\Psi\rangle_{\rm Zn}$ and can smoothly evolve into the latter under a weak local perturbation. So it is reasonable for one to take (12) as a good variational form for the zinc problem.

Since the holons are Bose-condensed in the superconducting and spontaneous vortex phases which we are concerned, A^h_{ij} in the spinon Hamiltonian (2) can be simplified as approximately describing a uniform flux with a strength

$$\sum\nolimits_{\Box} A^h_{ij} \simeq \pi\delta \tag{13}$$

per plaquette.

Under the condition (13), the spinon Hamiltonian H_s in (2) can be straightforwardly diagonalized as[18]

$$H_s = \sum_{m,\alpha} E_m \gamma^\dagger_{m\alpha}\gamma_{m\alpha} + \text{const.}, \tag{14}$$

by a Bogoliubov transformation

$$b_{i\sigma} = \sum_m w_{m\sigma}(i) \left(u_m \gamma_{m\alpha} - v_m \gamma^\dagger_{m-\alpha} \right) \tag{15}$$

with $|u_m| = \sqrt{\frac{\lambda+E_m}{2E_m}}$ and $|v_m| = \sqrt{\frac{\lambda-E_m}{2E_m}}$. A detailed treatment of this mean-field state in a self-consistent way can be found in Refs.[18,21].

Based on the above mean-field description, the zinc-free RVB ground state $|\Psi_0\rangle$ is defined by $\gamma_{m\alpha}|\Psi_0\rangle = 0$. Now we construct the states with one zinc being added to the system as discussed at the beginning of this section.

Firstly, according to the sudden approximation, the trial state with a zinc at site i_0 may be obtained by annihilating a *bare* spinon at site i_0 with a spin index, say, $-\sigma$:

$$|\Psi_0\rangle_{\rm Zn} = b_{i_0-\sigma} |\Psi_0\rangle . \tag{16}$$

Then, we allow the bosonic RVB order parameter Δ^s_{ij} to be adjustable around the zinc site to further minimize the total energy. Thus the final trial Zn state can be constructed in the following form

$$|\Psi\rangle_{\rm Zn} = C b_{i_0-\sigma} \left|\Psi_0[\Delta^s_{ij}]\right\rangle . \tag{17}$$

Here C is a normalization constant and $\left|\Psi_0[\Delta^s_{ij}]\right\rangle$ is the ground state of the Hamiltonian (2) under a fixed form of the RVB order parameter Δ^s_{ij}, which will generally deviate from the uniform Δ^s (of the pure system) around the zinc site.

In order to address the dynamic and thermodynamical properties, one needs to further determine the elementary excitations based on $|\Psi\rangle_{\rm Zn}$ defined in (17). We take the following steps to make the construction. Firstly, by using the Bogoliubov transformation (15), one has

$$\begin{aligned} C b_{i_0-\sigma}\left|\Psi_0\right\rangle &= C\sum_m w_{m\sigma}\left(i_0\right) v_m \gamma^\dagger_{m\sigma}\left|\Psi_0\right\rangle \\ &\equiv f^\dagger_{0\sigma}\left|\Psi_0\right\rangle, \end{aligned} \tag{18}$$

with $f^\dagger_{0\sigma} = C\sum_m w_{m\sigma}\left(i_0\right) v_m \gamma^\dagger_{m\sigma}$ and $C \equiv \left(\sum_m \left|w_{m\sigma}\left(i_0\right)\right|^2 v_m^2\right)^{-1/2}$. Secondly, define a new class of single spinon creation operators $f^\dagger_{n\sigma}$ as a linear combination of $\gamma^\dagger_{m\sigma}$'s, which satisfies

$$f^\dagger_{n\sigma} = \sum_m F^\sigma_{nm}\gamma^\dagger_{m\sigma},\ \sum_m \left(F^\sigma_{lm}\right)^* F^\sigma_{nm} = \delta_{l,n} \tag{19}$$

with $F^\sigma_{0m} \equiv C v_m w_{m\sigma}\left(i_0\right)$ such that $f^\dagger_{0\sigma}$ is consistent with the definition in (18). A proper F can be then obtained by re-diagonalizing the Hamiltonian (14): $H_s = \sum_{n\neq 0,\alpha}\widetilde{E}_n f^\dagger_{n\alpha}f_{n\alpha}$ + const., under a constraint $\sum_\alpha f^\dagger_{0\alpha}f_{0\alpha}=1$, with $\tilde{E}_n$ as the 'renormalized' spectrum in the presence of a zinc impurity.

Then the ground state with a zinc is simply given by $|\Psi\rangle_{\rm Zn} = f^\dagger_{0\sigma}\left|\Psi_0\right\rangle$ and the orthogonal (mean-field) excitation states are constructed by the creational operators $f^\dagger_{n\sigma}$ $(n\neq 0)$ as follows

$$\left|\{\nu_{n\alpha}\}\right\rangle_{\rm Zn} \equiv \prod_{n(\neq 0),\alpha}\left(f^\dagger_{n\alpha}\right)^{\nu_{n\alpha}}\left|\Psi\right\rangle_{\rm Zn}. \tag{20}$$

where $\nu_{n\alpha}$ denotes the occupation number at the state labelled by (n,α).

Physically, $f^\dagger_{0\sigma}$ in this approach is treated as a projection operator, from the original ground state to the zinc-doped ground state, while $f^\dagger_{n\alpha}$ $(n\neq 0)$ creates spinon excitations which are ensured to be orthogonal to $|\Psi\rangle_{\rm Zn}$. The presence of a zinc impurity at site i_0 will be enforced by the constraint $\sum_\alpha f^\dagger_{0\alpha}f_{0\alpha}=1$.

Finally, it is noted that instead of treating Δ^s_{ij} as unrestricted parameters in $\left|\Psi_0[\Delta^s_{ij}]\right\rangle$, we shall assume a simple site-dependence for Δ^s_{ij} ($ij\in$ nn sites) in the following variational calculation, which is given by

$$\left(\Delta^s_{ij}\right)_{nn} = \Delta^s\left[1-\left(1-p_0\right)e^{-\frac{\left(|i-i_0|+|j-i_0|\right)^2}{4R^2}}\right]. \tag{21}$$

Here the bulk value Δ^s is decided self-consistently in the zinc-free system[18,21]. The zinc at site i_0 will influence $\left(\Delta^s_{ij}\right)_{nn}$ within a radius R with p_0 determining the strength. The Lagrangian multiplier λ in the mean-field Hamiltonian (2) will be kept at the zinc-free value to ensure that the state remains the same at distances far away from the zinc site. The parameter p_0 will be decided by enforcing the global constraint for the total spinon number:

$$\sum_{i,\alpha}\left\langle b^\dagger_{i\alpha}b_{i\alpha}\right\rangle = N(1-\delta)-1 \tag{22}$$

[compared to (3)] in the presence of a zinc impurity with a given R.. In the following, most of results will be discussed for the case of $R=1$, i.e., within the sudden approximation, and then the stability of the results will be checked by allowing the variation of R.

IV. PHYSICAL CONSEQUENCES

Based on the above-constructed ground state and excited states, we can straightforwardly calculate various related physical properties, in the presence of a zinc impurity, by using the mean-field scheme similar to the pure system. The results are presented below.

Local $S=1/2$ moment.—As noted before, the ground state $|\Psi\rangle_{\rm Zn}$ defined in (17) differs from the pure state $|\Psi_0\rangle$ by a spin 1/2. The change of the spinon distribution around the zinc in the ground state (17) is numerically determined, as illustrated in Fig. 2, where the hole concentration is fixed at $\delta=0.125$, with the lattice size 16×16 and $R=1$ chosen in (21). Compared to the zinc-free mean value $1-\delta$ at a distance far away from the zinc site, the local density of spinons changes within a finite length scale near the zinc site as shown in Fig. 2, which accounts for the distribution of an unpaired spinon of $S=1/2$ in (17) created by the zinc substitution. Note that the spinon density is enhanced in the sublattice opposite to that of the zinc site, indicating that the unpaired spinon mainly stays there which reflects the fact that the underlying bosonic RVB pairing in (17) only involves spins at different sublattices[21]. It implies an AF spin configuration induced around the zinc as shown below.

Staggered moments.—Corresponding to the above spatial distribution of the $S=1/2$ moment, staggered (AF) moments are further shown in Fig. 3 around the zinc site. Note that the spin rotational symmetry breaking in Fig. 3 is because we fix $-\sigma=\downarrow$ in $|\Psi\rangle_{\rm Zn}$ such that the total spin change upon a zinc substitution is $\Delta S^z = 1/2$. The state $|\Psi\rangle_{\rm Zn}$ in general is a spin doublet according to its definition in (17) (if $|\Psi_0\rangle$ is spin singlet). The length scale ξ_{Zn} for the distribution of the local AF moments is essentially decided by the spin-spin correlation length in the original RVB ground state, $\xi_s \approx a\sqrt{2/\pi\delta}$(Ref.[21]). Fig. 4 shows the doping dependence of the scale ξ_{Zn} for the distribution of the local spin moments, defined by fitting $\langle S^z_i\rangle \simeq (-1)^i S_0 \exp(-|i-i_0|^2/\xi^2_{Zn})$. Indeed we find $\xi_{Zn}\simeq\xi_s$. For a hole doping $\delta=0.125$, $\xi_{Zn}\simeq 2.22a$. For a typical zinc doping in experiment, $\delta_{Zn}=0.03$, the average distance between two zincs is $d_{Zn}\approx a/\sqrt{\delta_{Zn}} = 7.07a$,

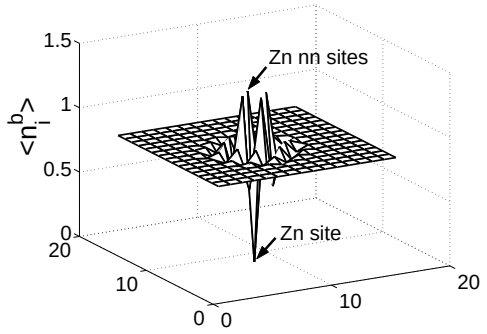

FIG. 2: Spinon density distribution $\langle n_i^b \rangle = \left\langle \sum_\sigma b_{i\sigma}^\dagger b_{i\sigma} \right\rangle$ around the zinc impurity. The lattice is 16×16 with doping $\delta = 0.125$.

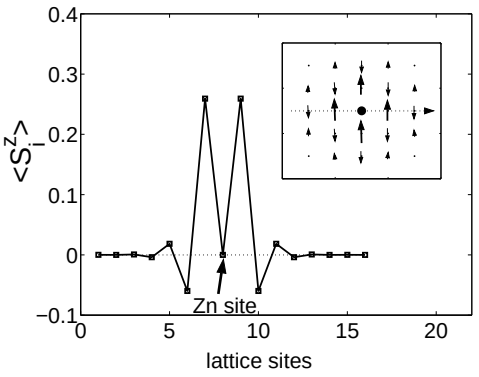

FIG. 3: The distribution of $\langle S_i^z \rangle$ near the zinc impurity, with the scan along the dashed direction shown in the inset, where the zinc site is marked by the filled circle.

which is larger than ξ_{Zn} at $\delta = 0.125$. In this dilute case, the correlation effect among different zinc impurities can be neglected and one may only focus on the single zinc effect.

Low-energy spin excitations.—One can further examine the dynamic properties of the induced local AF moments. One physical quantity is the spin-lattice relaxation rate of ^{63}Cu measured in NMR/NQR experiments, which is decided by the imaginary part of the spin correlation function $\chi(q,\omega)$ as follows

$$\frac{1}{^{63}T_1T} = \sum_q \frac{A^2(q)\,\mathrm{Im}\,\chi(q,\omega_N)}{\omega_N}\bigg|_{\omega_N \to 0} \qquad (23)$$

Here the structure factor $A(q) = A + 2B(\cos q_x a + \cos q_y a)$ and $A = -4B$ when the applied magnetic field is orthogonal to the CuO_2 plane[1]. So the main contribution will come from the AF correlations near the AF momentum (π,π). Fig. 5 shows the theoretical calculations. In the pure system of the bosonic RVB state, a pseudogap opens up in the spin excitations, resulting a suppression of $1/^{63}T_1T$

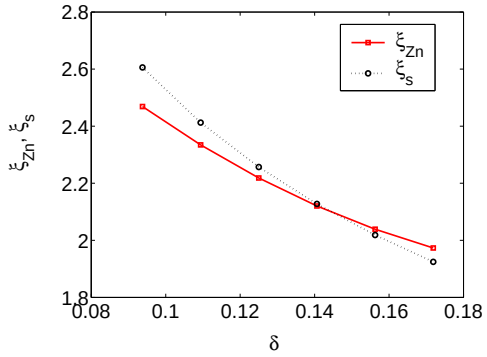

FIG. 4: The size of the spatial distribution of the local moments, ξ_{Zn} (solid), and the bulk spin correlation length, $\xi_s = \sqrt{2/\delta\pi}$ (dotted), vs. doping δ.

at low temperature (solid line with crosses in Fig. 5). However, for the zinc-doped system, the 'spin gap' shown in Fig. 5 is filled up by a Curie-type contribution, $1/^{63}T_1T \propto 1/T$, due to the presence of a free moment with a staggered distribution around the zinc site. The spatial distribution of $1/^{63}T_1T$ is given in Fig. 6 at a low temperature ($T = 0.0067J$), which clearly shows that the Curie-type signals are located near the zinc site, with its maximum at the nn sites of the zinc, consistent with the distributions of the staggered moments in Fig. 3.

It is noted that the calculation is performed at a 16×16 lattice with only one zinc, with an effective zinc doping concentration equal to $1/256 \sim 0.004$. In the realistic case with more zinc impurities, the intensity of $1/^{63}T_1T$ on average is expected to be proportional to the density of zinc impurities at low temperatures, so long as the zinc concentration is not too large such that the single-zinc approximation used above is still valid. Thus one should multiply a factor $5 \sim 8$ to the low-temperature part of $1/^{63}T_1T$ for the averaged case in Fig. 5 (solid curve with squares) in order to compare with the experimental case with $\delta_{\mathrm{Zn}} = 0.02 \sim 0.03$.

Furthermore, the uniform spin susceptibility can be directly calculated by $\chi_u \propto \mathrm{Re}\,\chi(q=0,\omega\to0)$.. χ_u also show a pseudogap behavior at low temperatures in the pure state, which is replaced by the Curie-like $1/T$ behavior near the zinc site due to the contribution from the local moment as shown in Fig. 7.

Dynamic spin susceptibility. —The imaginary part of the dynamic spin susceptibility, $\mathrm{Im}\,\chi(q,\omega)$, can be directly measured by inelastic neutron scattering. In the bosonic RVB mean field theory, a resonance peak at the AF wave vector $Q_{\mathrm{AF}} = (\pi,\pi)$ is present in the dynamic spin correlation function in the superconducting phase. For the hole doping $\delta = 0.125$, we obtain the resonance energy $E_g \approx 0.53J$[21]. Upon the zinc doping, the energy E_g of the resonance peak has changed little (see Fig. 8) in the bulk. But a zinc impurity does induce some new states at lower energies as shown in Fig. 8, which reflects

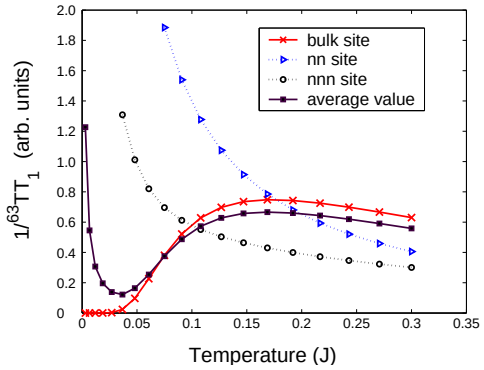

FIG. 5: Contributions to $1/^{63}T_1T$ from different sites are calculated. Solid curve with crosses: from the site far from the zinc impurity; Dashed curve with triangles: the nn site near the zinc; Dashed curve with circles: the next nearest neighbor (nnn) site near the zinc; Solid curve with squares: average over all sites in a 16×16 lattice with one zinc (see text).

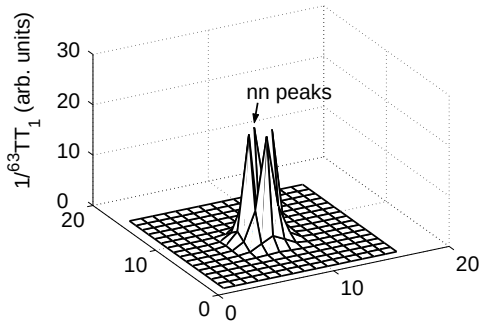

FIG. 6: Distribution of the contributions to $1/^{63}T_1T$ from individual sites near the zinc impurity, at temperature $T = 0.0067J$.

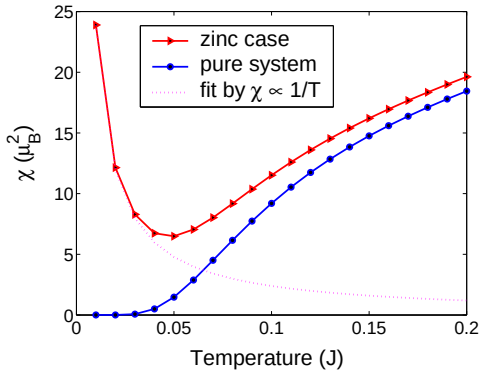

FIG. 7: Uniform spin susceptibility in the pure system is shown by the solid curve with full circles; The case with one zinc is illustrated by the solid curve with triangles; The dashed curve is a fit by $\chi = 0.2390/T$.

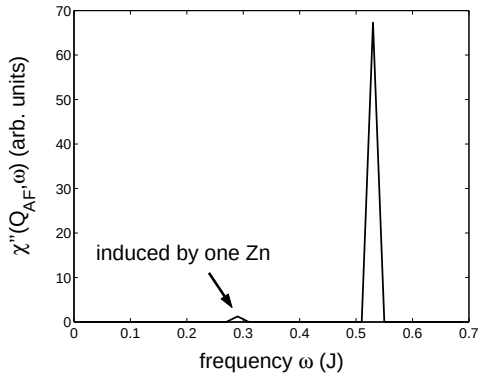

FIG. 8: Dynamic spin susceptibility at AF wavevector $Q_{\rm AF} = (\pi, \pi)$ with $\delta = 0.125$. The high-energy resonancelike peak at $E_g \simeq 0.53J$ is from the bulk (zinc free) state, while the low-energy excitations indicated by the arrow are new ones induced by the zinc impurity.

the modified spin excitation spectrum near the zinc, accompanying the emergence of a local moment. Note that the weight of such zinc-induced modes in Fig. 8 should be enhanced with a finite concentration of the zincs.

Effect from the holon redistribution.—So far the mean-field results are obtained based on the assumption that the Bose condensed holons are uniformly distributed in space. But in the presence of a zinc, the holon density near the zinc impurity should be generally suppressed, to be consistent with that the spinon density increases around the zinc site due to the no double occupancy constraint. In the bosonic RVB theory, since the holons will influence the spinon part by the gauge field A^h_{ij} defined in (8), the suppression of the holon density around a zinc will cause additional effects on the local spin dynamics, which is considered below.

As shown in Fig. 9, the intensity of the zinc-induced low-energy spin excitations seen in Fig. 8 will be enhanced with its energy scale further reduced if a holon density reduction is taken into account with a profile given by the inset. Meantime, the local staggered moments will also be increased (Fig. 10) under the same holon distribution. Although the above calculations are not based on a self-consistent scheme, which is generally quite difficult, all the important features found previously in the uniform profile of the holon distribution are kept unchanged qualitatively, except for that the anomalies are further strengthened due to the reduction of the holons which makes the area near the zinc closer to the half-filling.

Local stability of the mean-field theory.—The stability of the results discussed above based on the conjectured ground state (17) can be further examined by tuning the variational order parameter defined in (21). By changing the parameter R, the range of the zinc effect on the RVB parameter $\left(\Delta^s_{ij}\right)_{\rm nn}$ in (21) can be continuously adjusted. As shown in Fig. 11, the superexchange energy $\langle \tilde{H}_J \rangle_{\rm Zn}$

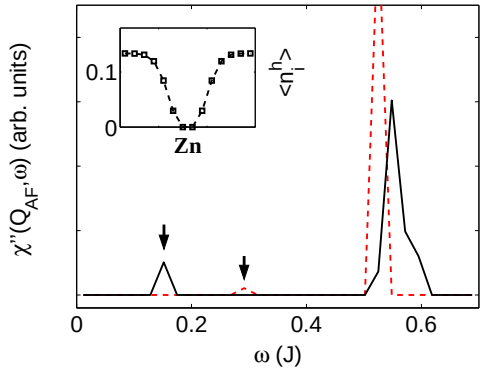

FIG. 9: Dynamic spin susceptibility at $Q_{\rm AF} = (\pi, \pi)$ is shown as the solid curve when the holon density is suppressed locally around the zinc (see the inset). For comparison, the dashed curve illustrates the case for a uniform holon density distribution.

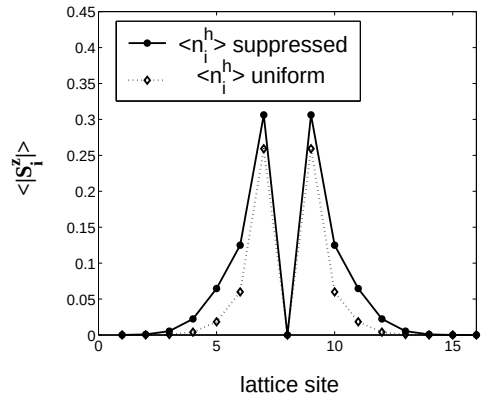

FIG. 10: The distribution of $|\langle S_i^z \rangle|$, corresponding to the profile of the holon density shown in the inset of Fig. 9, is plotted as the solid curve, as compared to the dashed curve for the uniform holon distribution.

is found to monotonically grow with the increase of R for both uniform and non-uniform profiles of the holon distribution, indicating that the sudden approximation state $|\Psi_0\rangle_{\rm Zn} \simeq |\Psi(R=1)\rangle_{\rm Zn}$ remains locally stable, which prevents the local $S = 1/2$ moment from leaking far away from the zinc impurity. When the holon redistribution discussed above is considered (see the dashed curve in Fig. 11), this local stability is further strengthened, since the frustration effect on the spin dynamics, which comes from the holon motion, is weakened around the zinc impurity due to the reduction of the holon density.

V. CONCLUSION

In this paper, we have developed a microscopic description of the zinc doping effect in the cuprate superconductors based on an effective theory, *i.e.,* the bosonic

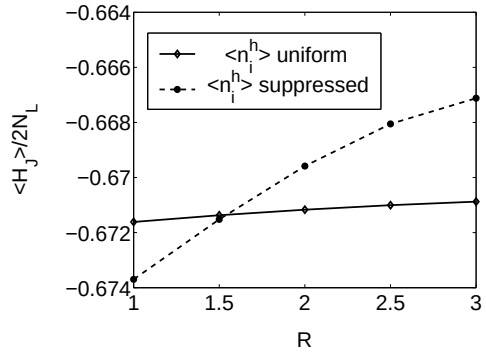

FIG. 11: The average superexchange energy $\langle H_J \rangle/(2N_L)$ per bond (N_L denotes the total number of lattice sites excluding the zinc sites) as a function of the parameter R in (21). Solid curve: uniform holon distribution. Dashed curve: locally suppressed holon density around the zinc indicated by the inset of Fig. 10.

RVB theory, of the $t-J$ model. The unusual effects of the zinc doping observed in the experiments have been explained as a direct consequence of the mutual nonlocal entanglement between the spin and charge degrees of freedom (*i.e.,* the phase string effect) in the doped Mott insulator. Once a local moment is formed due to such a topological mechanism, the effect of zinc doping can be simply described by a 'sudden approximation', which directly translates the short-range RVB pairing, present in the spin background state of the pure system, to the AF spin distribution around a zinc impurity, once the latter is introduced to the system. The NMR spin relaxation rates, uniform spin susceptibility, and the induced low-lying spin excitations, obtained within the sudden approximation and beyond, have consistently painted a unified picture of spin correlations near the zinc, which is shown to be stable locally and in an overall agreement with the experimental observations. In particular, the theory predicts that the range of the distribution for the local moment is inversely proportional to the square root of doping concentration.

In this work, an important property in the zinc problem has not been discussed so far. That is the behavior of quasi-particle excitations and the single-electron tunnelling properties. In the bosonic RVB theory, an electron is composed of a holon and a spinon, together with a nonlocal phase string factor[22]. In the superconducting phase, it has been shown[22] that a quasi-particle is stable due to a confinement of these holon-spinon and phase-string objects. So the overall low-energy single-particle spectral function is expected to be the same as in a d-wave BCS theory. However, the composite structure is predicted to be seen at high-energies, which may explain the 'coherent peak' in the antinodal regime in the pure system as due to the spinon excitation[22]. In the zinc doping case, due to the trapping of a free moment (spinon) near the zinc, the high-energy spinon contribu-

tion in the single-particle spectral function can become a zero-biased mode. Detailed study of this property needs the knowledge about the charge degree of freedom as well as the confinement in the superconducting phase, which is beyond the scope of this work. This issue and other problems, like how the superconducting transition temperature will be affected by the local moments, will be further investigated within the bosonic RVB description in future.

Acknowledgments

We acknowledge helpful discussions with W. Q. Chen, Z. C. Gu, T. Li, H. Zhai, F. Yang and Y. Zhou. The work is supported by the NSFC grants, and the grant no. 104008 and SRFDP from MOE of China.

[1] M.-H. Julien, T. Fehér, M. Horvatić, C. Berthier, O.N. Bakharev, P. Ségransan, G. Collin and J.-F. Marucco, Phys. Rev. Lett. **84**, 3422 (2000).
[2] A. V. Mahajan, H. Alloul, G. Collin, and J.-F. Marucco, Phys. Rev. Lett. **72**, 3100(1994); Eur. Phys. J. B **13**, 457 (2000).
[3] W. A. MacFarlane, J. Bobroff, H. Alloul, P. Mendels, N. Blanchard, G. Collin, and J.-F. Marucco, Phys. Rev. Lett. **85**, 1108, (2000).
[4] G. V. M. Williams and S. Krämer, Phys. Rev. B **64**, 104506 (2001).
[5] Y. Itoh, T. Machi, C. Kasai, S. Adachi, N. Watanabe, N. Koshizuka, and M. Murakami, Phys. Rev. B **67**, 064516 (2003).
[6] S. H. Pan, E. W. Hudson, K. M. Lang, H. Eisaki, S. Uchida and J. C. Davis, Nature **403**, 746 (2000).
[7] T. Kluge, Y. Koike, A. Fujiwara, M. Kato, T. Noji, and Y. Saito, Phys. Rev. B **52**, R727 (1995)
[8] A. V. Balatsky, M. I. Salkola, and A. Rosengren, Phys. Rev. B 51, 15547 (1995); M. I. Salkola, A. V. Balatsky, and D. J. Scalapino, Phys. Rev. Lett. **77**, 1841 (1996)
[9] N. Nagaosa, P. A. Lee, Phys. Rev. Lett. **79**, 3755 (1997)
[10] A. Polkovnikov, S. Sachdev, and M. Vojta, Phys. Rev. Lett. **86**, 296 (2001)
[11] G.-M. Zhang, H. Hu, and L. Yu, Phys. Rev. B **66**, 104511 (2002).
[12] J. X. Zhu, D. N. Sheng, and C. S. Ting, Phys. Rev. Lett **85**, 4944 (2000).
[13] Z. Q. Wang, P. A. Lee, Phys. Rev. Lett **89**, 217002 (2002).
[14] Hiroki Tsuchiura, Yukio Tanaka, Masao Ogata, Satoshi Kashiwaya, Phys. Rev. Lett. **84**, 3165 (2000).
[15] Y. Sidis, P. Bourges, and B. Hennion, L. P. Regnault, R. Villeneuve, G. Collin, J. F. Marucco, Phys. Rev. B **53**, 6811 (1995).
[16] R. S. Howland and T. H. Geballe, S. S. Laderman, A. Fischer-Colbrie, M. Scott, J. M. Tarascon and P. Barboux, Phys. Rev. B **39**, 9017 (1989).
[17] Z. Y. Weng, D. N. Sheng, Y.-C. Chen, and C. S. Ting, Phys. Rev. B **55**, 3894 (1997).
[18] Z. Y. Weng, D. N. Sheng, C. S. Ting, Phys. Rev. Lett., **80**, 5401(1998); Phys. Rev. B **59**, 8943 (1999).
[19] V. N. Muthukumar and Z. Y. Weng, Phys. Rev. B **65**, 174511 (2002); Z.Y. Weng and V.N. Muthukumar, Phys. Rev. B **66**, 094509 (2002).
[20] Q.H. Wang, Phys. Rev. Lett. **92**, 057003(2004); Chinese Phys. Lett. **20**, 1582 (2003).
[21] W. Q. Chen and Z. Y. Weng, preprint (2004).
[22] Y. Zhou, V. N. Muthukumar, and Z.-Y. Weng, Phys. Rev. B **67**, 064512 (2003); Z. Y. Weng, D. N. Sheng, C. S. Ting, Phys. Rev. B **61**, 12 328 (2000).